

Mineralogical And Chemical Characterisation Of The Iron- And Titanium-Bearing Phases In The Red Mud From The Rusal/Friguia Plant (Republic Of Guinea), With A View To Their Recovery.

Keita Kandas, Briton Bi Gouesse Henri, Kaba Ousmane Djene,
S.A. Sidoine Bonou

Laboratoire De Recherche Appliquée En Géosciences Et Environnement, Institut Supérieur Des Mines Et Géologie De Boké (République De Guinée)

Laboratoire Des Procédés Industriels De Synthèse, Environnement Et Energies Nouvelles (Lapisen), Institut National Polytechnique Houphouët Boigny De Yamoussoukro (Côte D'ivoire)

Laboratoire Des Techniques Aux Rayons X (X-Techlab), Agence De Développement De Sèmè City, O1bp 2028

Abstract

Red mud, a residue produced by the Bayer process during the conversion of bauxite into alumina, poses a major environmental challenge due to its high alkalinity and the large volumes generated. At the same time, it presents an opportunity for economic recovery thanks to the presence of valuable metals. Against this background, this study aims to characterise in detail the mineralogical and chemical properties of the iron (Fe)- and titanium (Ti)-rich phases contained in the red mud from the Rusal/Friguia plant in Guinea.

The methodological approach is based on a combination of complementary analytical techniques, notably X-ray fluorescence spectrometry (XRF), scanning electron microscopy (SEM) and X-ray diffraction (XRD), enabling the identification of the overall chemical composition as well as the crystalline phases present. The analyses reveal a predominance of iron-bearing phases, mainly haematite (Fe_2O_3), as well as the presence of titanium-bearing phases, confirming the mineralogical complexity of these residues.

The results obtained highlight significant concentrations of iron (36.6–38%) and titanium (2.7–3.3%), suggesting a gradual enrichment of these elements during the industrial process. These concentrations give red muds considerable potential for the recovery and utilisation of these strategic metals, particularly from the perspective of a circular economy and the reduction of environmental impacts associated with their storage. This study thus contributes to a better understanding of the potential for utilising red muds in Guinea.

Keywords : Red mud, iron, titanium, mineralogical characterisation, recovery, Rusal/Friguia, Guinea.

Date of Submission: 09-04-2026

Date of Acceptance: 19-04-2026

I. Introduction

The Republic of Guinea holds nearly two-thirds of the world's bauxite reserves and produces around 80 million tonnes per year, making it the world's leading player in the bauxite industry. In this context, the Rusal/Friguia plant is the country's main facility for processing bauxite into alumina, with a capacity of around 680,000 tonnes per year.

Bauxite, a lateritic rock first described by Pierre Berthier in 1821 at Les Baux-de-Provence, is mainly composed of aluminium and iron oxides (Agrawal and Dhawan, 2021). It is the main raw material for the production of alumina, a precursor to metallic aluminium, a strategic material widely used in the transport, construction and energy sectors due to its lightness and mechanical properties (Bouchard, n.d.).

However, the extraction of alumina using the Bayer process generates significant quantities of waste known as red mud. Globally, between 1.0 and 1.6 tonnes of waste are produced per tonne of alumina, amounting to over 66 million tonnes annually (Nguyen and Lee, 2018; Nie et al., 2020; Qu et al., 2023). These residues are characterised by high alkalinity resulting from the use of soda ash and lime, which complicates their environmental management and limits their revegetation (Hancock et al., 2023). Their storage in ponds also raises concerns regarding the stability of the embankments and the risks of dispersion of trace metallic elements such as vanadium, chromium or lead (Abdullah and Kamarudin, 2015; Kancir and Serdar, 2022; Zhang et al., 2020).

Despite these constraints, red mud constitutes a secondary deposit potentially rich in metals of interest such as iron and titanium, as well as critical elements such as scandium, gallium or vanadium (Agatzini-

Leonardou et al., 2008; Agrawal and Dhawan, 2021; Ujaczki et al., 2018). However, their complex mineralogical composition—including, in particular, hematite, goethite, anatase, quartz and various aluminosilicate phases—limits the efficiency of recovery processes (Li et al., 2023; Atakoglu and Yalcin, 2021; Ernilia et al., 2024). Although several studies have explored their utilisation in the metallurgical, cement or ceramic sectors, their industrial exploitation remains limited (Bonomi et al., 2016; Borra et al., 2015).

In this context, the mineralogical and chemical characterisation of the metal-bearing phases is a key step in guiding recovery strategies. In the case of the Rusal/Friguia plant, the gradual accumulation of red mud represents both an environmental challenge and a metallurgical potential that remains largely untapped.

This study therefore aims to characterise the mineralogical and chemical phases containing iron and titanium in the red mud from the Rusal/Friguia plant, in order to better understand their mode of occurrence and assess their potential for metallurgical recovery. Such an approach contributes to identifying more efficient recovery pathways for these metals whilst promoting the sustainable management of residues from the Bayer process in Guinea.

II. Materials And Methods

Sampling

Samples of red mud and bauxite were taken at the Rusal/Friguia plant site in Guinea. The bauxite was sampled at the inlet to the crushers, prior to the dissolution stage, whilst the red mud was taken from the residues produced by the Bayer process.

To ensure the representativeness of the analyses, a sampling campaign was carried out both upstream of the process and at the storage areas. Four composite samples were prepared from multiple individual samples to reduce the intrinsic heterogeneity of the material and obtain reliable and representative samples.

The samples studied fall into four categories:

- sludge from the sixth washer in the counter-current washing circuit, representative of the residues prior to their transfer to the storage yards;
- old sludge from the dam, corresponding to consolidated deposits that have undergone natural ageing;
- recent sludge from the dam, collected from the active deposition zones.
- raw bauxite, sampled at the inlet of the crushers prior to dissolution ;

All sampling points were georeferenced using GPS coordinates, thereby ensuring the traceability and reproducibility of the operations. This sampling strategy provides a suitable framework for a comparative analysis aimed at assessing the physico-chemical and mineralogical evolution of red mud, from its fresh state through to long-term storage. Photographs of these samples are shown in Figure 1.

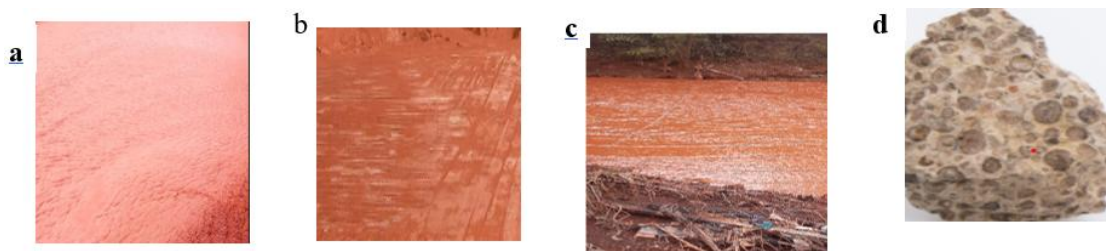


Figure 1 : Photos of the samples taken

Figure 1 (a, b, c and d) shows, respectively, the red sludge from the 6th Washer, old sludge, recent sludge and bauxite.

In order to better visualise and organise all the red mud sampling points, a sampling map was produced using ArcGIS software. This map allows the study sites to be precisely located and provides an understanding of the spatial distribution of the samples. It is shown in Figure 2.

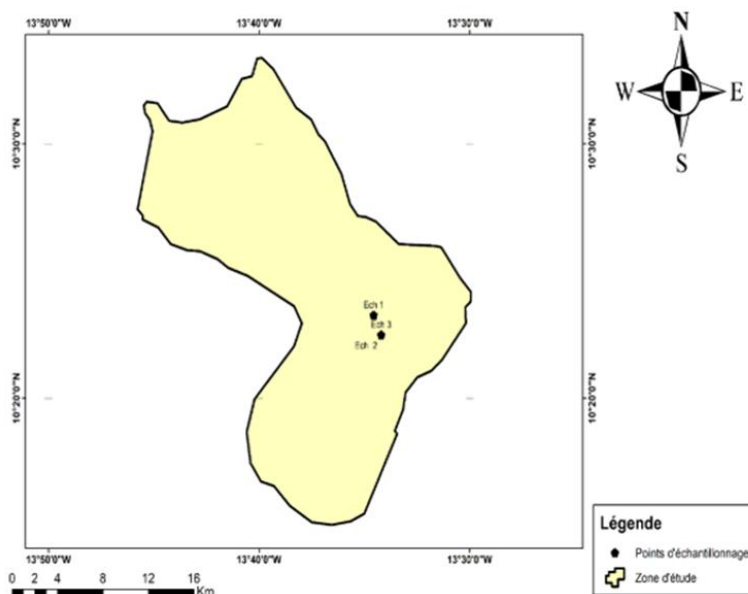


Figure 2: Sampling map of the three red mud samples collected

Analytical techniques

Samples of red mud from the storage pond at the Rusal/Friguia plant were collected and characterised in order to assess their potential for recovery of iron and titanium. The residual soda concentration was determined by acid-base titration, revealing values of 13.4 g/L, 11 g/L and 9 g/L, which exceed the industrial limit of 5 g/L.

To reduce the alkalinity, the sludge was washed with distilled water and then treated with an HX400 flocculant to improve settling. The solids were then vacuum-filtered, dried at 100 °C for 24 hours, and subsequently ground and sieved to obtain a fine, homogeneous powder. The final masses obtained were 3.500 kg, 2.970 kg and 1.650 kg respectively.

The samples were characterised using X-ray diffraction (XRD) to identify the mineral phases, scanning electron microscopy (SEM) for morphological analysis, and X-ray fluorescence (XRF) to determine the overall chemical composition. The SEM analyses were carried out at National Géosciences Research Laboratories (Nigéria), whilst the XRF analyses were carried out at the Félix Houphouët-Boigny National Polytechnic Institute in Yamoussoukro (Côte d'Ivoire).

III. Results And Discussion

Mineralogical characterisation

This stage enabled the precise identification of the various mineralogical phases present in the samples, as well as the characterisation of the morphologies associated with the crystalline structures. The analysis also contributed to a better understanding of the textural organisation of the minerals, their degree of crystallinity and their paragenetic associations. This information is essential for interpreting the physico-chemical behaviour of the materials, particularly during processing steps such as leaching, and for assessing their potential for recovery.

Mineralogical characteristics of the bauxite sample as determined by XRD

Indexing of the observed diffraction peaks reveals that the bauxite sample consists mainly of gibbsite, haematite, quartz and titanium dioxide in the anatase form. Figure 3 shows the indexed diffractogram of the bauxite sample, highlighting all the identified phases and their main crystallographic reflections.



Figure 8 : Photos du DRX

The mineralogy of the sample, dominated by gibbsite, confirms that it belongs to the group of lateritic bauxites rich in extractable alumina, in line with the literature, which highlights their suitability for the Bayer process due to their good solubility in an alkaline medium and their low-temperature digestion (Guozheng et al., 2020 ; Li et al., 2023 ; Mulchandani and Westerhoff, 2016). The significant presence of hematite also corresponds to conventional observations, where iron constitutes the main impurity, influencing the formation of red mud and representing both an industrial constraint and an opportunity for recovery (Karymsakova et al., 2024 ; Pepper et al., 2016 ; Srichandan et al., 2019).

Furthermore, accessory phases such as quartz and anatase play a significant role: quartz, which is not very reactive in its crystalline form, limits the impact on soda consumption, whilst titanium, which is stable and poorly soluble, is found predominantly in the residues. Thus, these results are consistent with the trends described in the international literature, highlighting a bauxite favourable for alumina extraction, but whose impurities require appropriate management and offer prospects for recovery.

Mineralogical characteristics of the recent red mud sample from the dam (BRB), as determined by XRD.

The diffractogram of the recent red dam sludge ('BRB') shows that the sample consists mainly of gibbsite, haematite, quartz, gypsum and rutile (TiO₂). The identification of these phases was confirmed by the agreement between the observed peaks and crystallographic references. Figure 4 shows the indexed diffractogram, highlighting all the phases present and their main reflections.

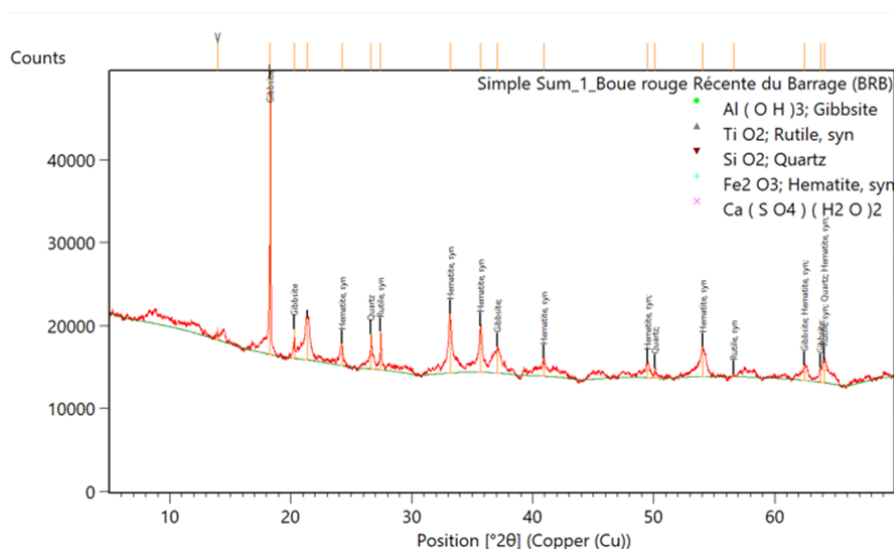


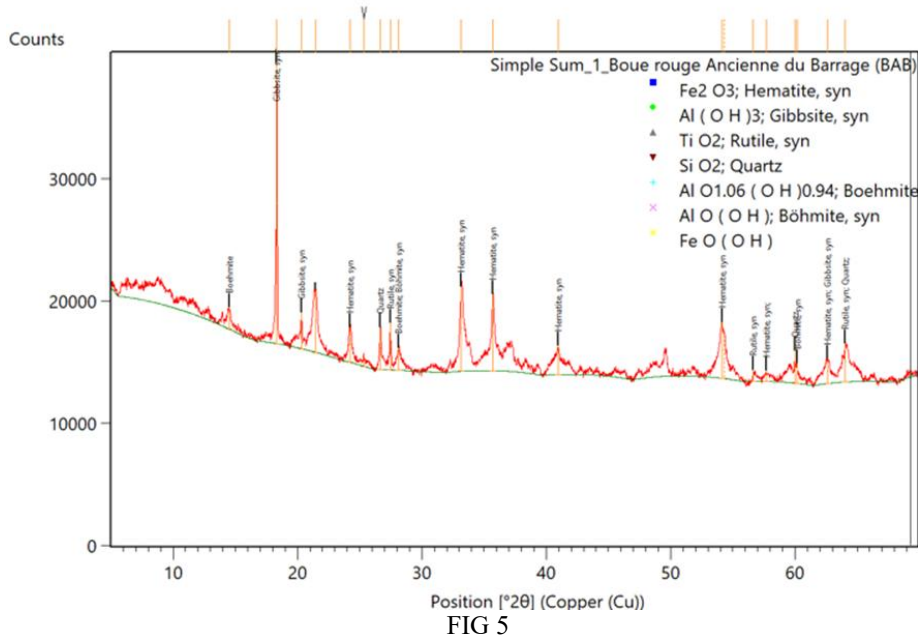
Figure 4 : Diffractogram of the sample of recent red mud from the dam

The results obtained are generally consistent with those reported in the literature on red muds from the Bayer process applied to lateritic bauxites. Indeed, the predominance of hematite as the main phase is well documented, reflecting the accumulation of insoluble iron oxides following alumina extraction. Previous work by Gao et al. (2019) also confirms that haematite constitutes the major phase, accompanied by resistant minerals such as quartz and rutile, due to their chemical inertness under the highly alkaline conditions of the process.

Furthermore, the residual presence of gibbsite in small proportions is consistent with the observations of several authors who attribute this persistence to kinetic limitations on dissolution or to entrapment within ferruginous or silicate matrices (Feng et al., 2022 ; Li et al., 2023). The formation of gypsum, although less systematically reported, has been observed in some recent studies, particularly in contexts of neutralisation or prolonged storage of red mud, where interactions with sulphate species may occur (Ernilia et al., 2024 ; Zhou et al., 2023). Finally, the detection of a minor amorphous or poorly crystallised phase is consistent with the findings of numerous studies indicating that red mud contains a significant amorphous fraction, resulting from the complex physico-chemical transformations undergone during processing and storage.

Mineralogical characteristics of the 'Old Red Mud from the Dam' (BAB) sample, as determined by X-ray diffraction (XRD).

The diffractogram analysis of the 'Ancient Red Sludge from the Dam' (BAB) shows that the sample consists mainly of gibbsite and boehmite, reflecting the presence of alumina phases that are both crystallised and partially hydrated. The detection of haematite and goethite indicates a significant concentration of iron oxides, typical of old sludge where iron accumulates over time. The indexed diffractogram is shown in Figure 5.



The results obtained are consistent with observations reported in the literature regarding the behaviour of red mud during storage. The predominance of hematite confirms the long-term stability of iron oxides, as extensively documented in studies on Bayer process residues. The presence of goethite is also frequently reported in older sludges, where it results from secondary weathering processes, notably through hydration or partial transformation of ferric phases under the influence of environmental conditions (humidity, temperature) (Barz et al., 2013 ; Panda et al., 2021).

Furthermore, the coexistence of gibbsite and boehmite reflects a gradual evolution of the alumina phases, consistent with studies showing dehydration and structural reorganisation during ageing (Wan et al., 2023). Quartz and rutile, as in other studies, remain stable and inert phases, concentrated in the residue. Finally, the presence of a poorly crystallised minor phase is consistent with common observations of an amorphous fraction in old red muds, indicating complex physico-chemical transformations and suggesting, as reported in several studies, a potential for metallurgical recovery that remains exploitable.

X-ray diffraction (XRD) analysis of the Red Mud sample from the 6th washer (B6L).

The diffractogram of the “6th washer mud” (B6L) reveals a composition dominated by gibbsite, hematite, and goethite, along with residual quartz and stable rutile. This mineralogy reflects the presence of aluminum hydroxides and iron oxides, as well as stable silicate and titanium-bearing phases, which are characteristic of red mud derived from industrial washing processes. Figure 6 shows the indexed X-ray diffraction (XRD) pattern of the “B6L” sample, highlighting the different identified mineralogical phases.

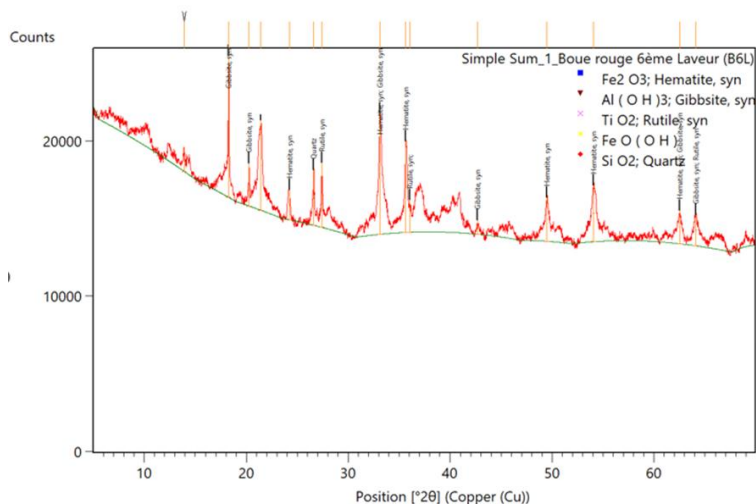


Figure 6: X-ray diffractogram of the red mud sample from the 6th washer

The analysis of the B6L sample shows a predominance of ferruginous phases, notably hematite (Fe_2O_3) and goethite ($\text{FeO}(\text{OH})$), illustrating the high stability of iron oxides and hydroxides after several washing cycles. Compared to the raw mud, this dominance is more pronounced, reflecting the progressive removal of soluble phases and the relative enrichment of iron in the residue (Karymsakova et al., 2024).

Gibbsite ($\text{Al}(\text{OH})_3$) appears in smaller quantities, indicating partial dissolution of soluble alumina, while quartz (SiO_2) and rutile (TiO_2) remain stable and inert, becoming relatively concentrated in the washed residues. These observations reflect a selective washing process, primarily aimed at removing soluble phases without affecting stable minerals (Atakoglu and Yalcin, 2021).

Finally, a low-intensity unindexed peak suggests the presence of a secondary phase or a partially crystallized amorphous phase.

Comparative analysis of the “Bauxite, BRB, BAB, and B6L” samples.

Figure 7 shows the superposition of the XRD diffractograms of the “Bauxite,” “BRB,” “BAB,” and “B6L” samples, allowing comparison of their mineralogical variations related to the transformations undergone during processing and washing.

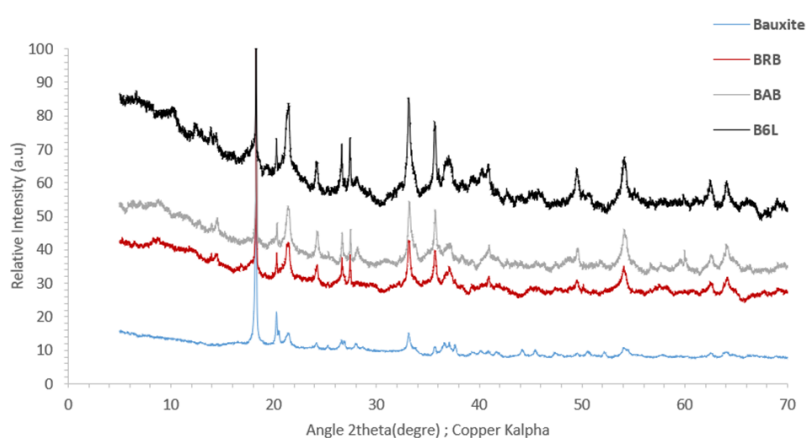


Figure 7: Superposition of XRD diffractograms of bauxite, BRB, BAB, and B6L samples

The superposition of the diffractograms highlights the coexistence of crystalline phases (gibbsite, hematite, quartz) and amorphous contributions, which are particularly pronounced in red mud and evolve with washing and aging.

Certain phases remain common and stable, such as quartz and titanium oxides (anatase/rutile), while transformations occur, notably the formation of boehmite in aged red mud, reflecting the evolution of alumina phases.

Overall, these results show that red mud retains phases rich in iron, aluminum, and titanium, confirming its potential as a valuable secondary resource.

Analysis of samples by Scanning Electron Microscopy (SEM)

The scanning electron microscopy (SEM) analysis of red mud reveals a morphological organization dominated by iron (Fe) and titanium (Ti) particles grouped in the form of aggregates, reflecting aggregation phenomena related to formation and precipitation processes. These SEM observations are presented in Figure 8.

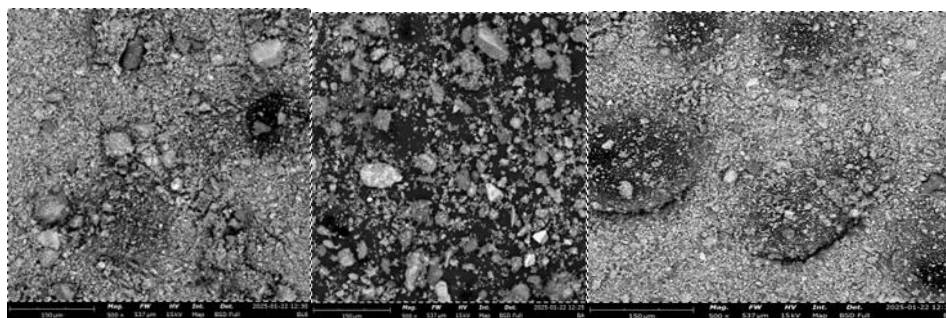


Figure 8: SEM micrographs of the observed samples

Figure 8 (a, b, and c) respectively depict the red mud from the 6th washer, aged red mud, and recent red mud.

The microstructural observations obtained are in good agreement with previous studies on red mud, which generally describe a heterogeneous texture characterized by aggregates of fine particles, variable porosity, and a broad particle size distribution. As in many studies, the predominance of iron and aluminum, along with the presence of silicon, titanium, and sodium, confirms the chemical complexity of Bayer process residues and their organization into a matrix dominated by ferric (hematite, goethite) and titanium-bearing (rutile) phases (Taneez and Hurel, 2019 ; Xiao et al., 2024 ; Arun et al., 2022 ; Barz et al., 2013). The dark, iron-rich zones observed in the SEM are also frequently reported, indicating localized segregation of iron oxide-rich phases.

Moreover, the aggregate morphology observed is consistent with literature descriptions, where red mud exhibits flocculated or agglomerated structures resulting from precipitation and storage conditions. Contrary to some hypotheses suggesting a limiting effect on extraction processes, several studies indicate, as in the present case, that this organization does not necessarily hinder performance but strongly influences reaction kinetics and mass transfer mechanisms (Abdinagoro and Hamsal, 2023 ; Bailly, 2024 ; Banga and Balsa-Canto, 2008 ; Boni et al., 2013 ; Deng et al., 2018). Therefore, accounting for these microstructural characteristics is essential to optimize treatment processes (leaching, solid/liquid separation), as highlighted in various recent studies on the valorization of red mud.

Chemical characterization by X-ray fluorescence (XRF)

X-ray fluorescence (XRF) analyses revealed that the red mud contains high levels of iron (36.6–38%) and titanium (2.7–3.3%). The graphical representations of these elemental analyses, shown in Figures 11 and 12, demonstrate the potential for recycling these residues for various industrial applications. The chemically characterized composition opens promising prospects for their valorization, particularly in the context of recycling processes or the extraction of valuable metals.

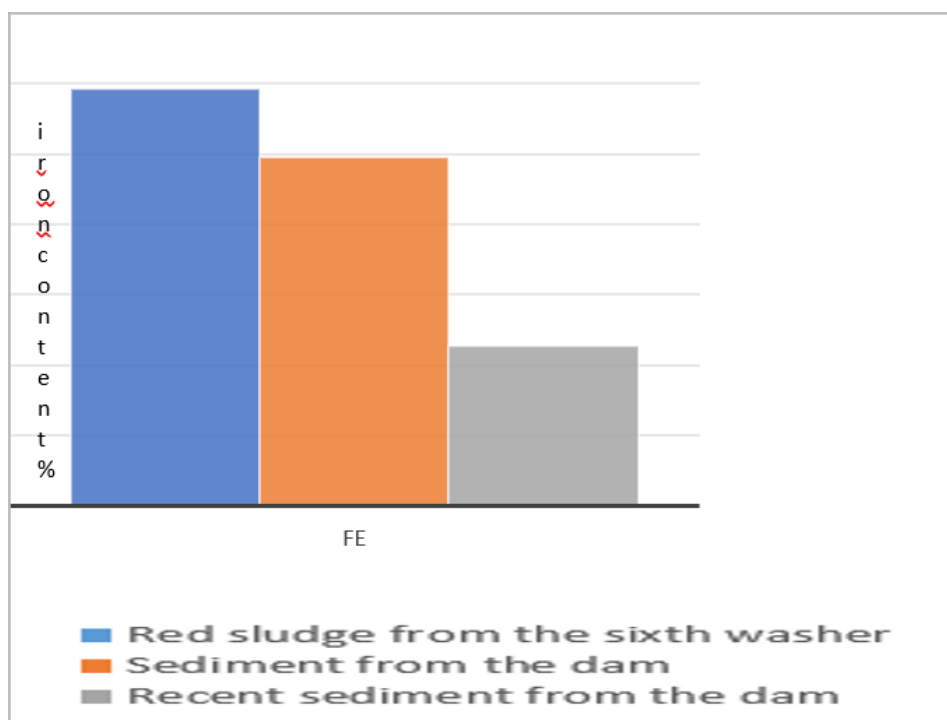


Figure 9: Histogram of iron content in red mud (%)

The results show that sample 1, from the sixth washing stage, has a higher iron content, reflecting a progressive enrichment in iron-bearing phases during the process. This accumulation is explained by the low solubility of iron-rich minerals, such as hematite and goethite, under alkaline conditions, which promotes their concentration in the solid residue. These observations are consistent with several previous studies (Abdinagoro and Hamsal, 2023; Deng et al., 2018; Liu et al., 2021; Malam et al., 2024; Rai et al., 2020; Wang et al., 2023; Ziental et al., 2020), which highlight the influence of treatment conditions on iron redistribution in red mud. However, the variations between samples reveal mineralogical heterogeneity linked to the processing parameters. Furthermore, although all samples show potential for iron recovery, extraction efficiency depends not only on the overall content, but also on the nature of the carrier phases and their degree of release, which can limit yields despite high concentrations.

Figure 10 shows the histogram of titanium content in red mud, determined by X-ray fluorescence (XRF).

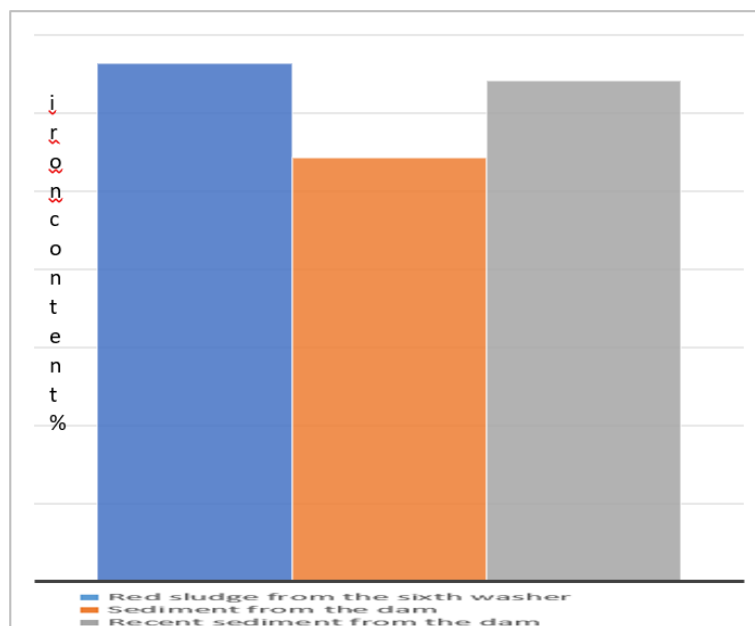


Figure 10: Histogram of titanium content in red mud (%)

Analysis shows a higher titanium content in sample 1 (sludge from the 6th scrubber), reflecting a progressive enrichment in titanium-bearing phases during the Bayer process, due to their low solubility in alkaline media. Titanium, generally present as stable minerals such as rutile, thus accumulates in the residues, which explains the observed heterogeneous distribution. These results are consistent with previous work (Liu et al., 2021; Pallavi et al., 2022; Samouhos et al., 2013; Xiao et al., 2024; Yuan et al., 2024), which highlights the influence of operating conditions on the concentration of poorly soluble elements. However, although all samples have titanium extraction potential, yields depend heavily on the nature of the carrier phases, their particle size and their degree of release, which can limit valorization, particularly in the presence of fine or refractory phases.

IV. Potential For Appreciation

Several options for the recovery of red mud can be considered, given its high metal oxide content and potential for industrial reuse. Magnetic separation is an effective method for concentrating and extracting iron-bearing phases (primarily hematite), thereby enabling iron recovery and reducing the environmental impact of the residues (Samouhos et al., 2013 ; Xiao et al., 2024). Furthermore, acid leaching appears to be a promising technique for solubilizing and recovering high-value-added elements such as titanium, by optimizing operating parameters to improve extraction yields (Qu et al., 2023; Rai et al., 2020).

Furthermore, the residues from these processes can be valorized within a circular economy framework, particularly in the cement industry or as construction materials. Their incorporation, as a partial substitute for conventional raw materials, not only reduces production costs but also limits the environmental footprint of industrial processes, while ensuring satisfactory mechanical properties of the resulting materials (Abadel et al., 2023 ; Al-Fakih et al., 2023; Feng et al., 2022).

V. Conclusion

This study enabled the precise characterization of the iron- and titanium-bearing phases present in the red mud from Rusal/Friguia, highlighting their mineralogical distribution and their association with other phases such as aluminosilicates and oxides. The results confirm that these industrial residues, long considered waste, are in fact a strategic secondary resource for the recovery of high-value-added metals, notably iron (primarily in the form of hematite) and titanium (often associated with rutile or complex phases).

However, the complexity of the mineral matrix—characterized by the fine interlocking of phases and their narrow particle size distribution—requires the development of tailored, integrated processing methods, potentially combining physical techniques (magnetic separation, particle size classification) and hydrometallurgical techniques (selective leaching). The significant content of these elements offers strong potential for recovery, both economically and environmentally, by helping to reduce the volume of stored waste. With this in mind, it appears essential to continue research aimed at optimizing extraction parameters, improving metallurgical recoveries, and rigorously evaluating the technical-economic feasibility and environmental impact of the proposed processes, within a framework of sustainable development and the circular economy.

Acknowledgments

We extend our sincere thanks to the Ministry of Higher Education and Scientific Research of the Republic of Guinea for its ongoing institutional support, as well as to the General Directorate of the Higher Institute of Mining and Geology in Boké for its academic guidance and crucial logistical support in the completion of this work. We also express our deep gratitude to the African Center of Excellence for Mining and the Mining Environment (CEA-MEM) for its financial and material support, which greatly contributed to the quality and success of this study.

The authors express their deep gratitude for the support of X-TechLab, the experimental platform dedicated to the use of X-ray techniques for scientific and technological research, hosted by the Sèmè City Development Agency in Benin.

Conflicts of Interest

Il n'existe aucun conflit d'intérêt entre les autres en lien avec ce travail

Authors' Contributions

Kandas KEITA designed the study, prepared the samples, and drafted the manuscript; Briton Bi Gouessé HENRI supervised and validated the analyses as well as the final version of the manuscript; Ousmane Djènè KABA contributed to the interpretation of the results, and S.A. Sidoine BONOU performed the powder X-ray diffraction experiments, as well as data collection and processing.

Références Bibliographiques

- [1]. Abadel, A., Alghamdi, H., Alharbi, Y., Alamri, M., Khawaji, M., Abdulaziz, M., Nehdi, M., 2023. Investigation Of Alkali-Activated Slag-Based Composite Incorporating Dehydrated Cement Powder And Red Mud. *Materials* 16. <https://doi.org/10.3390/Ma16041551>
- [2]. Abdinagoro, S., Hamsal, M., 2023. Strategic Marketing Approach Of Indonesia Aluminium Mineral Industry: Upstream And Downstream Analysis. *The Winners*. <https://doi.org/10.21512/Tw.V23i2.9199>
- [3]. Al-Fakih, A., Nor, Z.M., Basha, S.I., Shaikh, N., Ahmad, S., Al-Osta, M., Aziz, Md.A., 2023. Characterization And Applications Of Red Mud, An Aluminum Industry Waste Material, In The Construction And Building Industries, As Well As Catalysis. *Chem. Rec.* 23. <https://doi.org/10.1002/Tcr.202300039>
- [4]. Arun, J., Nachiappan, S., Rangarajan, G., Alagappan, R.P., Gopinath, K., Lichtfouse, E., 2022. Synthesis And Application Of Titanium Dioxide Photocatalysis For Energy, Decontamination And Viral Disinfection: A Review. *Environ. Chem. Lett.* 21, 339–362. <https://doi.org/10.1007/S10311-022-01503-Z>
- [5]. Bailly, S., 2024. Industrie Minière : Un Nouveau Procédé Transforme Les Boues Rouges En Source De Fer [WWW Document]. *Pourlascience.Fr*. URL <https://www.pourlascience.fr/Sd/Chimie/https://www.pourlascience.fr/Sd/Chimie/Industrie-Miniere-Un-Nouveau-Procede-Transforme-Les-Boues-Rouges-En-Source-De-Fer-26129.Php> (Accessed 10.26.24).
- [6]. Banga, J., Balsa-Canto, E., 2008. Parameter Estimation And Optimal Experimental Design. *Essays Biochem.* 45, 195–209. <https://doi.org/10.1042/BSE0450195>
- [7]. Barz, T., Cárdenas, D., Arellano-García, H., Wozny, G., 2013. Experimental Evaluation Of An Approach To Online Redesign Of Experiments For Parameter Determination. *Aiche J.* 59, 1981–1995. <https://doi.org/10.1002/AIC.13957>
- [8]. Boni, M., Rollinson, G., Mondillo, N., Balassone, G., Santoro, L., 2013. Quantitative Mineralogical Characterization Of Karst Bauxite Deposits In The Southern Apennines, Italy. *Econ. Geol.* 108, 813–833. <https://doi.org/10.2113/ECONGEO.108.4.813>
- [9]. Deng, B., Li, G., Luo, J., Ye, Q., Liu, M., Rao, M.-J., Peng, Z., Jiang, T., 2018. Selective Extraction Of Rare Earth Elements Over Tio₂ From Bauxite Residues After Removal Of Their Fe-, Si-, And Al-Bearing Constituents. *JOM* 70, 2869–2876. <https://doi.org/10.1007/S11837-018-3130-7>
- [10]. Feng, L., Yao, W., Zheng, K., Cui, N., Xie, N., 2022. Synergistically Using Bauxite Residue (Red Mud) And Other Solid Wastes To Manufacture Eco-Friendly Cementitious Materials. *Buildings*. <https://doi.org/10.3390/Buildings12020117>
- [11]. Liu, J., Wu, P., Jiang, Y., Wang, X., 2021. Explore Potential Barriers Of Applying Circular Economy In Construction And Demolition Waste Recycling. *J. Clean. Prod.* <https://doi.org/10.1016/J.Jclepro.2021.129400>
- [12]. Malam, C., Moore, K., Diallo, P., 2024. Compound Criticality Of Bauxite Production: Implications For Sustainability And Trade Neo-Colonialism. *Geoenergy*. <https://doi.org/10.1144/Geoenergy2023-054>
- [13]. Pallavi, Joshi, S., Singh, D., Kaur, M., Lee, H.-N., 2022. Comprehensive Review Of Orthogonal Regression And Its Applications In Different Domains. *Arch. Comput. Methods Eng.* 29, 4027–4047. <https://doi.org/10.1007/S11831-022-09728-5>
- [14]. Qu, Z., Liu, Jiancong, Su, T., Zhu, S., Liu, Junzhen, Chen, Y., 2023. Effective Recovery Of Ti As Anatase Nanoparticles From Waste Red Mud Via A Coupled Leaching And Boiling Route. *Front. Chem.* 11. <https://doi.org/10.3389/Fchem.2023.1201390>
- [15]. Rai, S., Bahadure, S., Chaddha, M., Agnihotri, A., 2020. A Way Forward In Waste Management Of Red Mud/Bauxite Residue In Building And Construction Industry. *Trans. Indian Natl. Acad. Eng.* 1–12. <https://doi.org/10.1007/S41403-020-00100-2>
- [16]. Samouhos, M., Taxiarchou, M., Tsakiridis, P., Potiriadis, K., 2013. Greek “Red Mud” Residue: A Study Of Microwave Reductive Roasting Followed By Magnetic Separation For A Metallic Iron Recovery Process. *J. Hazard. Mater.* 254–255, 193–205. <https://doi.org/10.1016/J.Jhazmat.2013.03.059>
- [17]. Wang, Z., Pan, Z., Cheng, Z., Wang, Y., 2023. Research On Evaluation Indices And Calculation Method Of Experimental Design. *Qual. Reliab. Eng. Int.* 39, 1909–1934. <https://doi.org/10.1002/Qre.3337>
- [18]. Xiao, J., Cheng, R., Zhang, J., 2024. Collaborative Separation Of Nickel And Iron From Nickel Laterite Ore And Red Mud. *Sep. Sci. Technol.* 59, 896–908. <https://doi.org/10.1080/01496395.2024.2339869>
- [19]. Yuan, K., He, S., Yu, B., Qian, S., Wu, X., Li, W., Zhao, C., 2024. Synergistic Leaching Of Titanium, Aluminum, And Magnesium Components During Dilute Acid Pressure Treatment Of High-Titanium Blast Furnace Slag. *Molecules* 29. <https://doi.org/10.3390/Molecules29143336>
- [20]. Ziental, D., Czarczyńska-Goślińska, B., Młynarczyk, D., Głowacka-Sobotta, A., Stanisz, B., Gośliński, T., Sobotta, L., 2020. Titanium Dioxide Nanoparticles: Prospects And Applications In Medicine. *Nanomaterials* 10. <https://doi.org/10.3390/Nano10020387>